

A mechanical model of a non-uniform ionomeric polymer metal composite actuator

Mart Anton, Alvo Aabloo, Andres Punning and Maarja Kruusmaa

IMS Lab, Institute of Technology, Tartu University, Nooruse 1, Tartu 50411, Estonia

E-mail: Mart.Anton@ut.ee, Alvo.Aabloo@ut.ee, Andres.Punning@ut.ee and Maarja.Kruusmaa@ut.ee

Received 10 March 2007, in final form 19 December 2007

Published

Online at stacks.iop.org/SMS/17/000000

[Ascii/Word/SMS/sms245825/PAP](#)
 Printed 10/1/2008
[Spelling ?](#)
[Issue no](#)
[Total pages](#)
[First page](#)
[Last page](#)
[File name](#)
[Date req](#)
[Artnum](#)
[Cover date](#)

Abstract

This paper describes a mechanical model of an IPMC (ionomeric polymer metal composite) actuator in a cantilever beam configuration. The main contribution of our model is that it gives the most detailed description of the quasistatic mechanical behaviour of the actuator with a non-uniform bending at large deflections reported so far. We also investigate a case where part of an IPMC actuator is replaced with a rigid elongation and demonstrate that this configuration would make the actuator to behave more linearly. The model is experimentally validated with MuscleSheet™ IPMCs, purchased from BioMimetics Inc.

Q.1 (Some figures in this article are in colour only in the electronic version)

Nomenclature

w	Width of the IPMC sheet (m)
d	Thickness of the IPMC sheet (m)
l	Length of the free part of the IPMC sheet (m)
l_c	Length of the fixed part of the IPMC sheet (m)
l_F	Length of the free loaded IPMC section (m)
s	Natural parameter of the curve representing the IPMC sheet (m)
s_F	Position on the sheet where force is applied (m)
B	Bending stiffness (N m ²)
E	Equivalent Young's modulus (Pa)
F_{sheet}	Force applied to the sheet (N)
F	Force applied to the object (N)
ϕ	Angle between the normal of the sheet and the tangent of the trajectory (rad)
R	Radius of the trajectory (m)
p	Position of the object on the trajectory (m)
$k_0(s)$	Initial curvature (m ⁻¹)
$\hat{\alpha}_0$	Initial angular deflection in the position of the object (rad)
$k(s)$	Curvature (m ⁻¹)
$\alpha(s)$	Tangential angle (rad)
$\hat{\alpha}$	Angular deflection in the position of the object (rad)
$\vec{P}(s)$	Position vector (m)

\vec{P}	Position vector of the centre of the loaded section of the IPMC (m)
$M(s)$	Bending moment caused by force applied to the sheet (N m)
\bar{M}	Mean bending moment of the loaded section of the IPMC caused by force applied to the sheet (N m)
$M_e(s)$	Electrically induced bending moment (EIBM) (input voltage is unspecified) (N m)
$M_e^+(s)$	EIBM at +2 V (N m)
$M_e^-(s)$	EIBM at -2 V (N m)
M_e	Constant EIBM (input voltage is unspecified) (N m)
M_e^+	Constant EIBM at +2 V (N m)
M_e^-	Constant EIBM at -2 V (N m)
$\vec{T}(\theta)$	Tangent vector, where θ is tangential angle (unitless)
$\vec{N}(\theta)$	Normal vector, where θ is tangential angle (unitless)

1. Introduction

IPMC (ionomeric polymer metal composite) is a type of electroactive material that bends in an electric field [1, 2]. It consists of a thin swollen polymer film, such as Nafion™, filled with water or an ionic liquid. Both sides of the polymer film are plated with thin metal electrodes. Voltage applied between the surface electrodes causes migration of ions inside the structure of the polymer, which in turn causes the mechanical bending

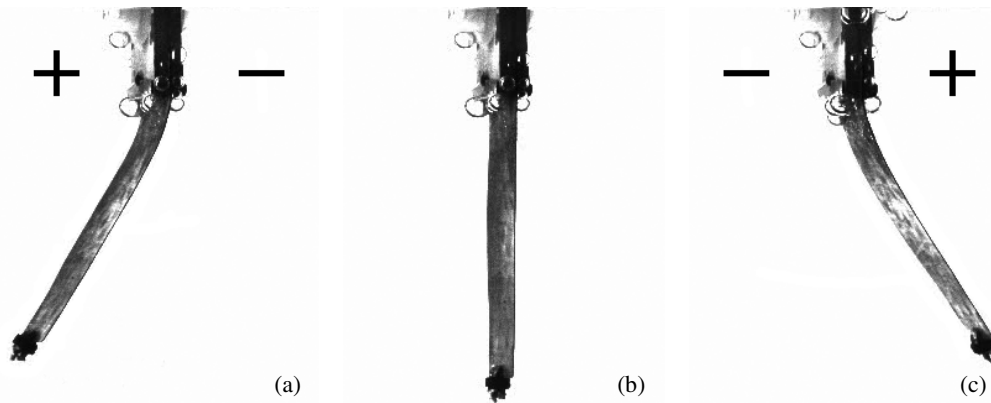


Figure 1. IPMC with ((a) and (c)) and without (b) electrical stimulation.

of the sheet, as shown in figure 1. The direction of bending depends on the polarity of the applied electric field.

This paper investigates the mechanical model of an IPMC sheet in the cantilever beam configuration. It is a physical model, with electrically induced bending moment (abbreviated as EIBM) as an input parameter and enables the calculation of the shape of the sheet.

Various mechanical and electromechanical models of IPMCs have been developed by a number of authors, emphasizing different features [3–11]. Table 1 summarizes the features usually considered in those models. Table 2 represents the comparison between our paper and previously described models of the IPMC. Besides the features depicted in the table the models can also differ in other details. For example, Tamagawa *et al* [3] describe the time-dependent behaviour of elasticity and EIBM, the model proposed by Sangki *et al* [6] is two-dimensional, while in all the other papers the load is crosswise to the beam and Pugal *et al* [11] considers the axial load.

The main motivation of our work is to develop a mechanical model of the IPMC actuator that, as precisely as possible, describes the quasi-static behaviour of IPMC cantilever beams. For example, we considered it to be important to describe the behaviour at large deflections and with varying load positions. It makes it possible to use the model for a large variety of applications. Also, we are interested in applying the model in the case of materials with various properties. For example, it is often the case that the model has an initial bending curvature or the EIBM varies along the surface, but only a few models consider these assumptions.

Another feature of our model is that it permits modelling an IPMC actuator with a rigid passive elongation. The reason for doing this is that we want to investigate how the elongation changes the behaviour of the actuator. In this paper we show that the elongation makes the behaviour of the actuator more linear and therefore easier to control.

Several models [3, 4, 7, 8] assume linear behaviour of the IPMC actuator. In our work we do not make such an assumption as it is rather restrictive. For example, it permits modelling the IPMC only at small deflections but we are also interested in cases where the bending is large and non-uniform.

Assuming nonlinear behaviour makes it possible to investigate a more general case. Furthermore, it makes it also possible to determine to what extent the behaviour of the IPMC can be linearized. In our paper we show that this is the case if, for example, a short sheet with a rigid elongation is considered.

The model presented in this paper permits comparing actuators with various properties. This would facilitate a general understanding of how the behaviour changes when the properties change and thus help in designing better actuators. In this paper we show the comparison of actuators with and without elongation. We allow EIBM to vary along the sheet and we also investigate the possibility that EIBM is constant.

The limitation of our model is that it does not consider viscoelasticity and other dynamic properties of IPMC cantilever beams. To elaborate the model so that it also accurately describes the dynamic behaviour of the sheet is a direction for future work.

The remainder of this paper is organized as follows. In section 1 the system is described. Experiments are discussed in section 3. In section 4 the model is validated against experimental data. In section 5 possible applications and the direction of future work are discussed. Finally, concluding remarks are provided in section 6.

2. The model

This section represents the mechanical model of the IPMC cantilever actuator with the properties given above.

Our objective is to model a situation where an IPMC sheet in a cantilever configuration manipulates an object. The sheet can have an absolutely rigid elongation attached to the tip. In this paper we study quasi-static movements of the object. Thus, we model the sheet in a static equilibrium state.

A part of the IPMC sheet is fixed between contacts at clamps or the elongation. The mechanics of that part do not need to be modelled. The rest of the sheet can bend and is called the free part of the IPMC sheet. The length of the free part is l . Formally every IPMC sheet in this model has an elongation with an infinite length. It helps to model elongated sheets but can equally well be used for modelling sheets without an elongation.

Table 1. Features relevant to the modelling of IPMCs.

Feature	Description
1 Non-uniform bending	Is the curvature of the IPMC sheet assumed to be constant or not? In general only free bending curvature may be considered approximately constant. And even then only if EIBM is constant and the IPMC sheet is moving slowly. As soon as the IPMC sheet is loaded, the curvature will vary along the sheet.
2 Initial curvature	IPMC sheets may be initially curved even when neither force nor electric current is applied (see table 3). Alternatively the model may be suited to describe only nearly perfectly straight IPMC sheets.
3 Large deformations	In this paper all deformations that result in deflection angles larger than 90° are considered large. Models that do not support large deformations have a gradually increasing modelling error as the deflection angle approaches 90°.
4 Non-uniform EIBM	Several authors report that EIBM varies along the sheet [12–14]. Alternatively, in the case of small pieces of an IPMC, small currents and good electrode layers the EIBM can be considered uniform.
5 Force output	IPMC actuators can be used to apply force to an object (load cell). Alternatively only a free bending of the IPMC sheet may be modelled.
6 Varying load position	When the IPMC actuator pushes an object along a trajectory, it does work. So the IPMC sheet applies force to the object in different positions. Alternatively the force may be determined only on the same plane as the contacts.
7 Elongation	A rigid elongation may be attached to the top of the IPMC sheet. The advantages of that kind of construction are discussed in this paper.
8 Linearity	Can the model be defined by linear differential equations? Linearity is very important if we want to control the IPMC sheet in real time.
9 Dynamic behaviour	Does the model describe the movements of the IPMC sheet? Alternatively the model may only describe the static equilibrium of the IPMC sheet. This kind of model can be used to describe quasi-static movements of the sheet—movements that are so slow that inertial and drag forces can be neglected.

The shape of the IPMC sheet is modelled as a curve on a plane (see figure 2(a)). The curve (or the neutral curve) is a projection of the neutral surface of the sheet—the surface that neither contracts nor expands. The neutral surface is assumed to be cylindrical. The only allowed deformation is bending. The neutral curve is extended by a ray (see figure 2(a)) which represents the elongation.

Throughout this paper s denotes the natural parameter of the neutral curve that specifies a position on the sheet at a distance s from contacts along the curve. The neutral curve

is defined by its curvature $k(s)$ (see figure 2(b)). The curvature of the elongation $s > l$ is zero. The curvature of the IPMC part of the curve is given by

$$\forall s \leq l: \quad k(s) = k_0(s) + \frac{M_e(s) + M(s)}{B} \quad (1)$$

$k_0(s)$ is the initial curvature of the IPMC sheet, B is the bending stiffness and $M_e(s)$ is the electrically induced bending moment (EIBM). $M(s)$ is the bending moment caused by the force applied to the sheet. $M(s)$ is equal to the area of the parallelogram in figure 2(b).

The force applied to the sheet is F_{sheet} (see figure 2(b)). Then the force applied to the object is $-F_{\text{sheet}}$. The object needs not to be specified. The only thing we need to know is that the point of contact is located on a circular trajectory in a position p (see figure 2(b)). The centre of the circle is at the contacts of the sheet and the radius is R . The contact point on the neutral curve is s_F (see figure 2(a)).

The model can be used for calculating the deflection angle $\hat{\alpha}$ at the position of the object. In general there is no simple analytical formula for that. Please refer to [15] for the corresponding numerical algorithm. However, if we assume that EIBM is constant ($M_e(s) = M_e$) it holds that

$$\hat{\alpha} = \hat{\alpha}_0 + \frac{l_F \cdot (M_e + \bar{M})}{B}, \quad (2)$$

where

$$l_F = \min(l, s_F), \quad (3)$$

$\hat{\alpha}_0$ is the initial angular deflection in the position of the object and \bar{M} is the mean bending moment (see figure 2(a)). Please refer to appendix B for derivation of (2).

The mean bending moment \bar{M} caused by an external force is equal to the bending moment in the centre of the bendable section— \vec{P} (see figure 2(a)). \bar{M} can be calculated with

$$\bar{M} = \|(\vec{P}(s_F) - \vec{P}) \times (F_{\text{sheet}} \cdot \vec{N}(\hat{\alpha}))\|, \quad (4)$$

where $\vec{P}(s_F)$ points to the location of the object (see figure 2(c)) and $F_{\text{sheet}} \cdot \vec{N}(\hat{\alpha})$ is the force vector applied to the sheet. Please refer to appendix C for the derivation of (4).

Equations (1) and (2) are the basic equations of the model. Please refer to appendix A for the complete list of equations which define the model.

Our further objective is to calculate the quasi-static work done by moving an object along the arc. The sheet is assumed to be in frictionless contact with the object, thus reaction $-F_{\text{sheet}}$ is perpendicular to the sheet. To calculate the output work, we need to find the force component F (see figure 2(b)) that is in the direction of the tangent of the arc. For the rest of the paper, if we talk about force we mean F . The force is given by

$$F = -F_{\text{sheet}} \cdot \cos(\phi), \quad (5)$$

where ϕ is the angle between the forces $-F_{\text{sheet}}$ and F (see figure 2(b)).

If we double the width of the IPMC sheet, it is equivalent to two sheets working in parallel. The force needed to bend it would double. The same holds for stiffness and EIBM.

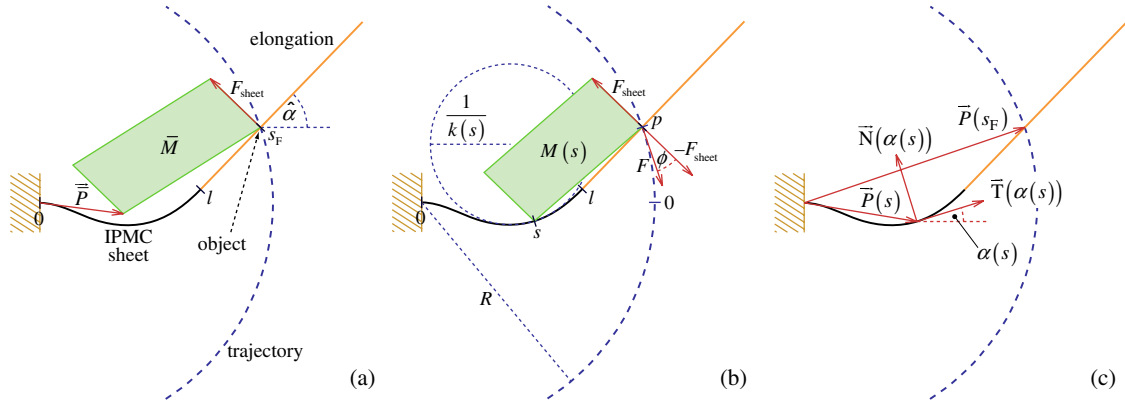


Figure 2. Geometric definitions of the parameters.

Table 2. Comparison of the authors’ model with those from the literature on the basis of whether they address the features in table 1.

Feature	Paper										
	This	[3]	[4]	[5]	[6]	[7]	[8]	[9]	[10]	[11]	
1 Non-uniform bending	✓	✓	✓	✓	✓	✓		✓		✓	
2 Initial curvature	✓								✓		
3 Large deformations	✓			✓				✓	✓		
4 Non-uniform EIBM	✓							✓			
5 Force output	✓	✓	✓	✓	✓	✓	✓				
6 Varying load position	✓			✓	✓						
7 Elongation	✓						✓				
8 Linearity		✓	✓			✓	✓				
9 Dynamic behaviour			✓			✓		✓		✓	

The output force F , bending stiffness B and EIBM $M_e(s)$ are proportional to the width w of the sheet. B and $M_e(s)$, normalized to the width of the sheet, characterize the properties of the IPMC material.

The IPMC is a sandwich with a cracked surface and several layers with different elastic moduli. The Young’s modulus of a homogeneous sheet with the same dimensions and similar stiffness can be calculated using the equation

$$E = \frac{12 \cdot B}{w \cdot d^3}, \quad (6)$$

where d is the thickness of the IPMC sheet. For non-homogeneous material like IPMC this parameter is called the effective Young’s modulus or equivalent Young’s modulus. It can be used to characterize the properties of the IPMC material.

3. Experiments

This section describes the experiments conducted to verify the model introduced in the previous section and to compare actuators with and without elongation. First, the experimental set-up is discussed. Then experimental data is introduced.

3.1. Experimental set-up

The system set-up allows applying voltage to an IPMC sheet, with or without elongation, and to measure force and the

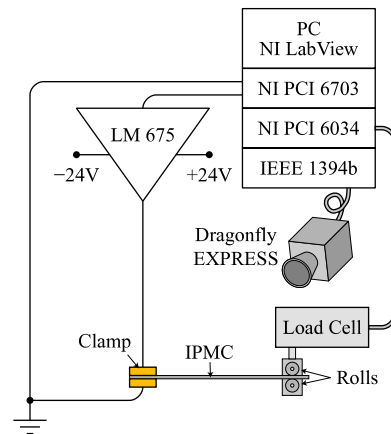


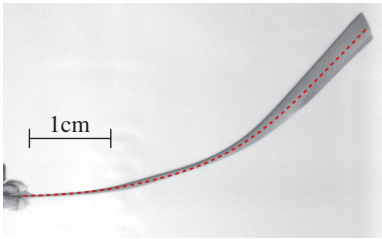
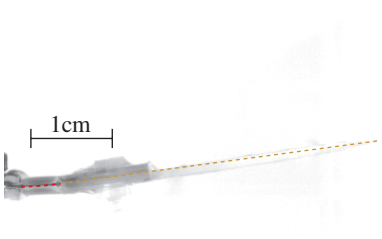
Figure 3. System set-up.

neutral curve in an arbitrary position of the object (in our case the load cell).

Our system consists of six basic parts (see figure 3):

- (1) A sheet either consisting entirely of an IPMC material or a combination of an IPMC material and a plastic elongation attached to it with a bolt and a nut.
- (2) A clamp for holding the sheet. The jaws of the clamp are made of gold and also serve as an electrical contact. They also hold the sheet so that it bends in the horizontal plane.

Table 3. Sheet configurations.

Configuration	Long IPMC sheet	Short IPMC sheet with the plastic elongation
Side view of the sheet and the initial neutral curve (the red line) with curvature— $k_0(s)$		
Length of the freely bending IPMC part— l	50 mm	4.5 mm
Length of the fixed part of the IPMC sheet— l_c	1.5 mm	3.5 mm
Width of the IPMC sheet— w	11 mm	11 mm
Thickness of the IPMC sheet— d	0.21 mm	0.21 mm

Q.A

The horizontal motion ensures that gravity does not affect the experimental results.

- (3) A Transducer Techniques GSO-10 load cell is used to measure the force applied by the sheet. The maximum force that can be measured is about 0.1 N. The sheet is held between two rolls to achieve a frictionless contact. Between the experiments the load cell can be repositioned with respect to the clamp.
- (4) A black&white camera, Dragonfly EXPRESS, is used to record the sheet. The resolution of the camera is 640×480 pixels and the frame rate used is 25 fps. From the acquired images the neutral curve can be determined.
- (5) The inputs and outputs of the system are controlled and monitored with a PC running LabView 7. The input voltage of the sheet is controlled with a National Instruments I/O board PCI-6703. The load cell is attached to a DAQ board PCI-6034. The Dragonfly EXPRESS camera is connected to the IEEE 1394b port.
- (6) The control signals generated by the I/O board are amplified using the amplifier LM675 (National Semiconductor).

The IPMC used in the experiments is a commercial product of BioMimetics Inc., called MuscleSheet™ with Pt surface electrodes and Na + doping ions.

Table 3 summarizes the information about the two sheet configurations used in the experiments. The long IPMC sheet is initially twisted but will be straight when held between rolls. The short IPMC sheet is cut from the first part of the long IPMC sheet after conducting the experiments with the long one. The parameter l_c specifies the length of the IPMC sheet that is fixed between contacts at clamps or at the elongation. This parameter does not influence the behaviour of the sheet. Parameters w and d , on the other hand, have a direct impact on the sheet's behaviour. They are not explicitly used in the model but model parameters B and $M_e(s)$ are related to them. They are measured to assess the parameters of the IPMC material.

Throughout this paper we call the actuators 'long sheet' and 'short sheet', respectively. Throughout this paper the radius of the trajectory is $R = 40$ mm. In the experiments the

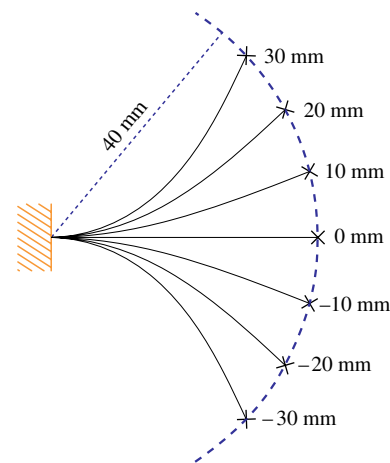


Figure 4. Positions on the trajectory where the force and shape of the sheet are measured. The measurement denotes the distance along the trajectory from position zero.

force is measured at seven positions located on the trajectory (see figure 4).

For each of the:

- two sheet configurations,
- seven trajectory positions and
- three driving voltages (+2, 0 and -2 V)

the force F and the neutral curve of the sheet are measured. From the neutral curve, the curvature $k(s)$ can be extracted.

3.2. Implementation details

For every sheet configuration and position of the trajectory the force and the neutral curve at three driving voltages (+2, 0 and -2 V) are measured. Voltage input and timing of important readings can be seen in figure 5. The corresponding output current can be seen in figure 6. The first ten readings are taken at 0 V. After these ten readings, the readings are taken alternately at +2 and -2 V. The force and the neutral curve are measured 0.5 s after the start of the impulse. To permit signal filtering the total length of the input pulse is 0.6 s.

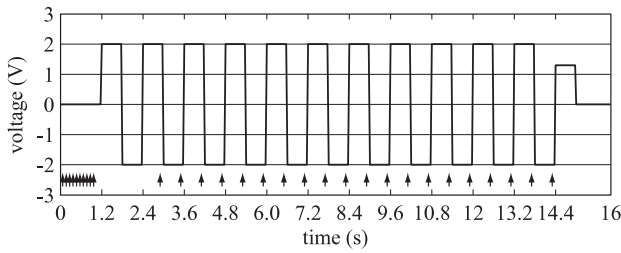


Figure 5. Input voltage and times of moments of important readings.

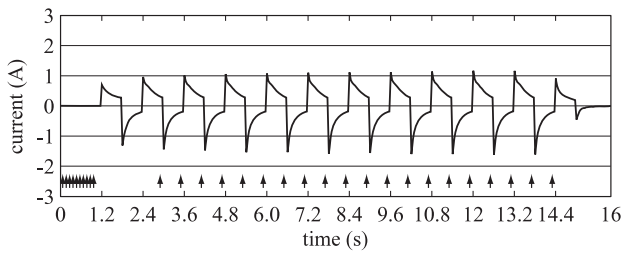


Figure 6. Output current in the case of the long IPMC sheet.

The electric current at 2 V dehydrates the IPMC sheet [1, 16]. Changes in the hydration level of the IPMC sheet cause changes in the bending stiffness and response to electrical stimulation. Therefore the experiments were kept as short as possible and the IPMC sheet was moistened between measurements.

After every pulse, water is unevenly distributed within the material. The first two pulses are neglected because initial conditions are different compared to those of the following pulses.

We measure the force component in the direction of the tangent of the trajectory. The load cell measures the component of the force that is perpendicular to it and has to be positioned perpendicular to the tangent of the trajectory. Ten readings are taken and the mean value is used as the result.

Ten images are saved synchronously with the force measurements. The mean of these images as light intensity matrices is computed. This operation may cause motion blur.

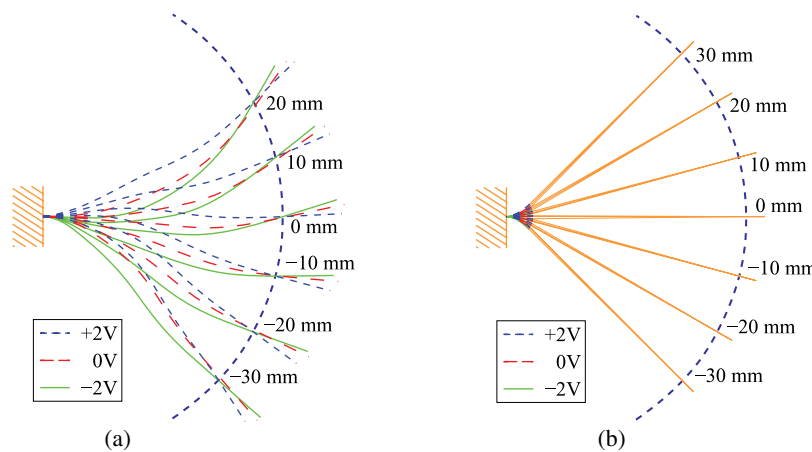


Figure 7. Neutral curves of the long sheet (a) and the short sheet (b).

The neutral curve of the IPMC part of the sheet is interpolated with a minimum variation curvature curve [17]. The curvature of such a curve can be easily revealed analytically.

3.3. Experimental data

Figure 7 represents the neutral curves measured. Measured forces are presented in figure 9. Please refer to [18] and [19] for the videos of the experiments of the long and the short sheet, respectively, in a position of the trajectory $p = 0$.

In the videos [18, 19] and in figure 7 it can be seen that, with different voltages, the static equilibrium state of the sheet differs. In the case of a long sheet the difference is large. In the case of a short sheet with an elongation the difference is barely noticeable. When considering moving sheets the shape of the sheet is an input parameter that we need to know in order to calculate the output force. In the case of a short sheet with elongation the shape of the sheet does not vary so much and can be easily estimated. In the case of the long sheet estimation of the shape of the sheet is more difficult.

Readings of the long sheet taken at a position +30 mm along the trajectory are invalid because the sheet systematically got stuck between the rolls.

4. Model validation

In this section we validate the model of the IPMC actuator by extracting the parameters for the model and comparing the simulation results with the experimental results of the previous section.

4.1. Parameter identification

The parameters that have to be extracted from the experiments for both of the sheet configurations are bending stiffness and the electrically induced bending moment (EIBM). Each of the three driving voltages used in the previous section causes a different EIBM: the bending stiffness, however, is always the same.

At 0 V $M_e = 0$ (no EIBM). The following equation derived from (2) can be used to calculate the bending stiffness:

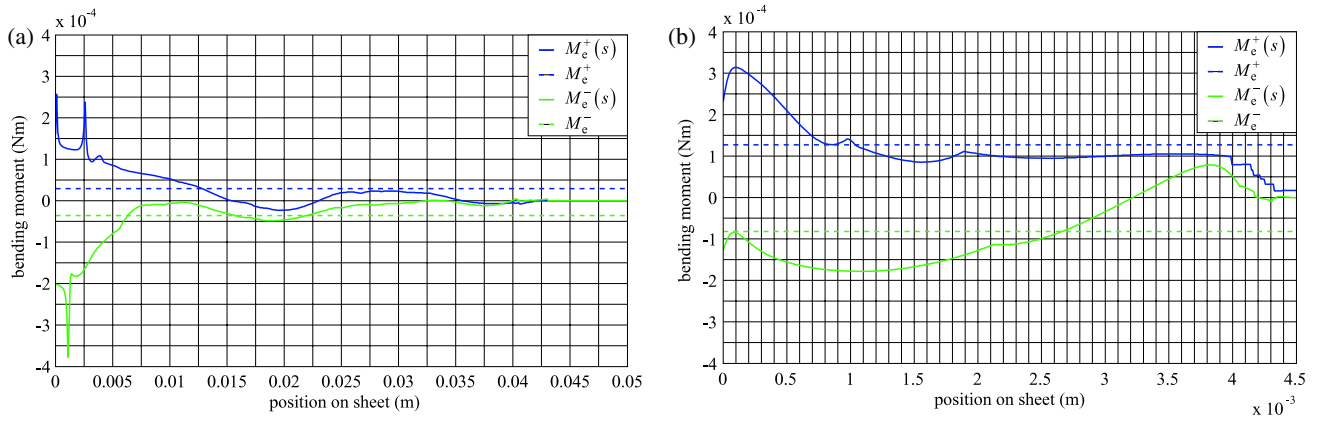


Figure 8. EIBM of the long sheet (a) and the short sheet (b).

Table 4. Extracted parameters.

Configuration	Notation (equation)	Long IPMC sheet	Short IPMC sheet
Bending stiffness	B	$2.03 \times 10^{-6} \text{ N m}^2$	$1.21 \times 10^{-6} \text{ N m}^2$
Bending stiffness normalized to the width of the sheet	$\frac{B}{w}$	$1.84 \times 10^{-4} \text{ N m}$	$1.10 \times 10^{-4} \text{ N m}$
Equivalent Young's modulus	E	236 MPa	147 MPa
Constant EIBM at +2 V	M_e^+	0.029 mN m	0.127 mN m
Constant EIBM at -2 V	M_e^-	-0.036 mN m	-0.082 mN m
The mean absolute value of constant EIBM	$\frac{M_e^+ - M_e^-}{2}$	0.032 mN m	0.104 mN m
The mean absolute value of constant EIBM normalized to the width of the sheet	$\frac{M_e^+ - M_e^-}{2w}$	2.95 mN	9.47 mN

$$B = \frac{l_F \cdot \bar{M}}{\hat{\alpha} - \hat{\alpha}_0}. \quad (7)$$

There are a number of measurements (corresponding to different positions on the trajectory) that each give a sample of the bending stiffness. The weighted average is used as the result. A weighting coefficient \bar{M} is used so that the experiments with a higher mean bending moment would contribute more to the result.

The varying EIBM in the case of both electrical stimulations can be calculated using an equation derived from (1):

$$M_e(s) = B \cdot (k(s) - k_0(s)) - M(s). \quad (8)$$

For calculating the constant EIBM the equation derived from (2) can be used:

$$M_e = \frac{B \cdot (\hat{\alpha} - \hat{\alpha}_0)}{l_F} - \bar{M}. \quad (9)$$

In both cases (varying and constant EIBM) there are again a number of measurements that each give a sample of EIBM. The arithmetical average is used as the result.

4.2. Identified parameters of the model

Extracted parameters are presented in table 4 and in figure 8.

Observations:

- (1) The long sheet appears to be stiffer than the short sheet (although the short IPMC sheet is cut from the first part of the long IPMC sheet). This can be explained by changes in the hydration level [1, 16]. The short IPMC sheet is surrounded by water while the long sheet is not (for the side view of the sheet see table 3). The short IPMC sheet is surrounded by water because elongation is close to the contacts and because of the surface tension of water.
- (2) As s increases the varying EIBM tends to converge to zero. This can be explained by the fact that, when moving toward the top of the sheet, the potential between surfaces drops because of the surface resistance [12–14]. The smaller the potential is, the smaller is the EIBM.
- (3) The M_e^+ value for the long sheet is smaller than the M_e^+ for the short sheet. The same statement applies for the mean absolute value of a constant EIBM. It is a direct result of the effect introduced in the previous point.
- (4) EIBM (both varying and constant) at voltages +2 and -2 V do not have the same absolute value. This reflects the asymmetry of the material.
- (5) Varying EIBM changes polarity or has peaks at some positions. This is caused by errors in curvature measurements.

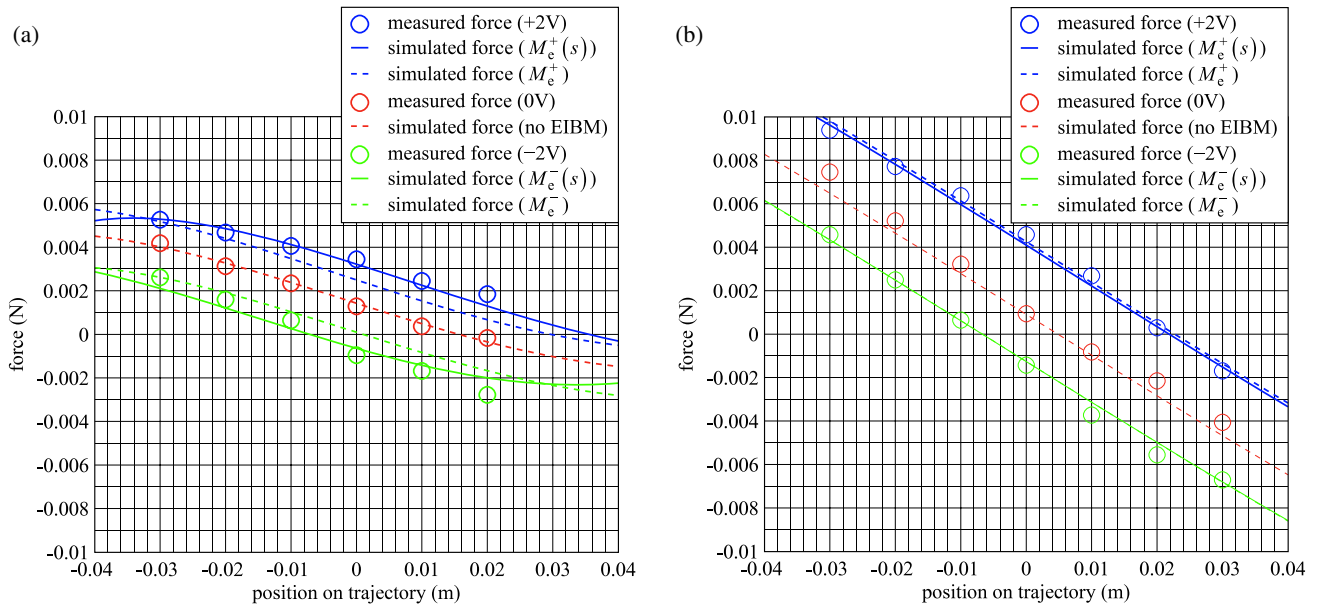








Figure 9. Real and simulated forces of the long sheet (a) and the short sheet (b).

Table 5. Real and simulated neutral curves and root mean squared errors at +2 V in position 0 m of the trajectory.

Configuration	Long IPMC sheet	Short IPMC sheet with plastic elongation
Actual	 RMSE = 0 mm	 RMSE = 0 mm
With varying EIBM.	 RMSE = 0.44 mm	 RMSE = 0.05 mm
With constant EIBM.	 RMSE = 2.23 mm	 RMSE = 0.09 mm

4.3. Simulations

With the parameters extracted in the previous section and the parameters from table 3 the simulations are conducted and the simulation results are validated against the experimental data.

The system of equations given in appendix A can be solved using a customized numerical integration technique. The challenge in our case is that, at first, we know only one point of the function we are integrating. The rest of the points are found in the course of integration. The algorithm is implemented in LabView 8.0. Please refer to [15] for documentation and source code.

Q.2

In figure 9 real and simulated output forces at different electrical stimulations can be seen. In table 5 real and simulated neutral curves at +2 V in position 0 mm of the trajectory can be seen. The root mean squared error of the neutral curve for the IPMC part of the sheet is also given.

Table 6 gives root mean squared errors of the neutral curve and of the output force over all positions of the trajectory.

Varying EIBMs ($M_e^+(s)$ and $M_e^-(s)$) are calculated with (6) based on curvature. Constant EIBMs (M_e^+ and M_e^-) are calculated with (7) based on the deflection angle. It is easier to measure the angle than the curvature but comparison of the experiments and simulations indicates that, in the case of the long sheet, the use of constant EIBM causes larger modelling errors (see table 6). In the case of the short sheet, the use of constant EIBM gives as good results as the use of varying EIBM does.

The position–force relation is linear in the case of the short sheet. This is important with respect to precision control of such an actuator. As controlling a linear time-invariant system (LTI) is very easy, stabilizing a nonlinear system (like the actuator with a long sheet) can be very difficult.

Table 6. Root mean squared errors over the neutral curve and output force over all positions.

Configuration		Long IPMC sheet	Short IPMC sheet with plastic elongation
Varying EIBM	Neutral curve	0.81 mm	0.13 mm
	Force	0.322 mN	0.424 mN
Constant EIBM	Neutral curve	2.13 mm	0.18 mm
	Force	0.622 mN	0.422 mN

The initial position of the object (without electrical stimulation) is 15 mm in the case of the long sheet and 5 mm in the case of the short sheet (see figure 9). The short sheet can apply more force in the initial position than the long sheet is able to. The main reasons are:

- most of the work is done by the IPMC material near the input contacts, where the bending moment caused by the external force is the largest and
- EIBM tends to converge to zero in the direction away from the contacts [12–14].

5. Possible applications and future work

The model presented and validated in this paper can be used to determine the properties of an actuator and to optimize the construction of the actuator.

To determine the properties of the actuator we need to know l , $k_0(s)$ and R . For every position p of the trajectory and for every EIBM $M_e(s)$ the model determines the shape of the sheet $k(s)$ and the force F applied to the object. Please refer to [15] for the corresponding algorithm.

Usually we are only interested in a specific section of the positions of the trajectory, the working section and a set of EIBMs determined by the material. Given the working section and a set of realistic EIBMs the model enables us to do the following:

- To find the linear fit of the force F as a function of p in the given working section. If the mean squared error is small enough the linear fit can be used for creating a linear controller.
- To find the maximal difference of the shapes of the sheet at the extreme opposite realistic EIBMs. The less the shape of the sheet varies, the easier it is to control it.
- To find the minimal length of the sheet, capable of reaching the object in every position of the working section.
- To find the maximal force that can be applied in the direction of the tangent and the normal of the trajectory.
- To find the maximal magnitude of the force that can be applied in both directions within the working section.

Furthermore, the model also enables us to find the minimal area of an IPMC sheet capable of applying a predefined force within a predefined working section. As the force per area

of the sheet does not depend on the width of the sheet, the required parameter is the optimal length of the IPMC sheet. After the optimal length is found, the width of the sheet can be chosen according to the required output force. To investigate how and when the elongation as a construction element improves the performance of the actuator and the optimal configuration of the actuator is the topic for future research.

6. Conclusions

We presented a model of a cantilever IPMC actuator with a varying electrically induced bending moment. We validate the model against two actuators: a long IPMC sheet and a short IPMC sheet with a rigid elongation. The experimental results show that, for the short sheet, the position–force relationship is linear whereas the position–force relationship of the long sheet is nonlinear.

This paper presents a static analysis of IPMC mechanics. It enables us to compute the free bending curvature and force applied to an object in a static equilibrium state. A dynamic model which considers motion, masses and viscoelasticity is a subject for future study. However, for cases where accelerations and velocities are small enough, the static model is shown to be accurate. It is also suitable for finding the optimal design of the actuator.

Acknowledgments

This work has been supported by the Estonian Information Technology Foundation and the Estonian Science Foundation (grant nos. 6765 and 6763).

Appendix A. Formal definition of the model

The relations between parameters are defined by the following equations:

$$\vec{T}(\theta) = (\cos(\theta) \quad \sin(\theta) \quad 0), \quad (10)$$

$$\vec{N}(\theta) = (-\sin(\theta) \quad \cos(\theta) \quad 0), \quad (11)$$

$$l_F = \min(l, s_F), \quad (12)$$

$$F = -F_{\text{sheet}} \cdot \cos(\phi), \quad (13)$$

$$\phi = \hat{\alpha} - \frac{p}{R}, \quad (14)$$

$$\vec{P}(s_F) = R \cdot \vec{T}\left(\frac{p}{R}\right), \quad (15)$$

$$k(s) = \begin{cases} k_0(s) + \frac{M_e(s) + M(s)}{B} & s \leq l \\ 0 & s > l \end{cases}, \quad (16)$$

$$\alpha(s) = \int_0^s k(u) du, \quad (17)$$

$$\hat{\alpha} = \alpha(s_F), \quad (18)$$

$$\hat{\alpha}_0 = \int_0^{l_F} k_0(u) du, \quad (19)$$

$$\vec{P}(s) = \int_0^s \vec{T}(\alpha(u)) du, \quad (20)$$

$$\vec{P} = \frac{1}{l_F} \cdot \int_0^{l_F} \vec{P}(u) du, \quad (21)$$

$$M(s) = \begin{cases} \|(\vec{P}(s_F) - \vec{P}(s)) \times (F_{\text{sheet}} \cdot \vec{N}(\alpha(s_F)))\| & s \leq s_F \\ 0 & s > s_F \end{cases}, \quad (22)$$

$$\vec{M} = \frac{1}{l_F} \cdot \int_0^{l_F} M(u) du. \quad (23)$$

For realistic results $l > 0$, $B > 0$, $R > 0$ and $-\frac{\pi}{2} < \phi < \frac{\pi}{2}$. To be able to use the cross product, all the vectors, except the result of the cross product, are three-dimensional with zero z coordinate.

Appendix B. Derivation of equation (2)

Assuming $M_e(s) = M_e$ from (1) we get

$$\begin{aligned} \forall s \leq l_F \quad k(s) &= k_0(s) + \frac{M_e + M(s)}{B} \Rightarrow \\ \int_0^{l_F} k(u) \cdot du &= \int_0^{l_F} \left(k_0(u) + \frac{M_e + M(s)}{B} \right) du \Leftrightarrow \\ \int_0^{l_F} k(u) \cdot du &= \int_0^{l_F} k_0(u) \cdot du \\ &+ \frac{l_F \cdot M_e + \int_0^{l_F} M(u) \cdot du}{B} \Leftrightarrow \\ \alpha(l_F) &= \hat{\alpha}_0 + \frac{l_F \cdot (M_e + \frac{1}{l_F} \cdot \int_0^{l_F} M(u) \cdot du)}{B} \Leftrightarrow \\ \alpha(s_F) &= \hat{\alpha}_0 + \frac{l_F \cdot (M_e + \vec{M})}{B} \Leftrightarrow \\ \hat{\alpha} &= \hat{\alpha}_0 + \frac{l_F \cdot (M_e + \vec{M})}{B}, \end{aligned}$$

Q.3 which is (2). Above we first integrate both sides of the equation. In the second step we use the linearity property of integration. In the third step we use (17) and (19). In the fourth step we use (16), (17) and (23). In the fifth step we use (18).

Appendix C. Derivation of equation (4)

From (23) we get

$$\begin{aligned} \vec{M} &= \frac{1}{l_F} \cdot \int_0^{l_F} M(u) du \\ &= \frac{1}{l_F} \cdot \int_0^{l_F} \|(\vec{P}(s_F) - \vec{P}(u)) \times (F_{\text{sheet}} \cdot \vec{N}(\alpha(s_F)))\| du \\ &= \left\| \left(\vec{P}(s_F) - \frac{1}{l_F} \cdot \int_0^{l_F} \vec{P}(u) \cdot du \right) \times (F_{\text{sheet}} \cdot \vec{N}(\hat{\alpha})) \right\| \\ &= \|(\vec{P}(s_F) - \vec{P}) \times (F_{\text{sheet}} \cdot \vec{N}(\hat{\alpha}))\|, \end{aligned}$$

which is (4). Above, the first equality is from (12) and (22), the second equality follows from the linearity of the cross product and integration and the third equality is from (21).

References

- [1] Nemat-Nasser S and Thomas C 2004 *Electroactive Polymer (EAP) Actuators as Artificial Muscles—Reality, Potential and Challenges* 2nd edn, ed Y Bar-Cohen (Bellingham, WA: SPIE) chapter 6, p 171
- [2] Shahinpoor M and Kim K J 2001 *Smart Mater. Struct.* **10** 819–33
- [3] Tamagawa H, Yagasaki K and Nogata F 2002 *J. Appl. Phys.* **92** 7614
- [4] Yagasaki K and Tamagawa H 2004 *Phys. Rev. E* **70** 052801
- [5] Bao X, Bar-Cohen Y, Chang Z and Sherrit Stewart 2004 Characterization of bending EAP beam actuators *Proc. SPIE Int. Soc. Opt. Eng.* **5385** 388–94
- [6] Sangki L, Hoon C P and Kwang J K 2005 *Smart Mater. Struct.* **14** 1363–8
- [7] Newbury K M and Leo D J 2003 *J. Intell. Mater. Syst. Struct.* **14** 333–42
- [8] Huynh N N, Alici G and Spinks G M 2006 Force analysis and characterization of polymer actuators *Proc. Int. Conf. on Intelligent Robots and Systems (Beijing)* pp 5465–70
- [9] Yim W, Trabia M, Renno J, Lee J and Kim K 2006 Dynamic modeling of segmented ionic polymer metal composite (IPMC) actuator *IEEE/RSJ Int. Conf. on Intelligent Robots and Systems (Beijing, China)*
- [10] González C and Llorca J 2005 *Int. J. Solids Struct.* **42** 1537–45
- [11] Pugal D, Kim K J, Punning A, Kasemägi H, Kruusmaa M and Aabloo A 2007 *J. Appl. Phys.* at press
- [12] Shahinpoor M and Kim J K 2000 The effect of surface-electrode resistance on the performance of ionic polymer–metal composite (IPMC) artificial muscles *Smart Mater. Struct.* **9** 543–51
- [13] Punning A, Anton M, Kruusmaa M and Aabloo A 2006 Empirical model of a bending IPMC actuator *Proc. SPIE* **6168** 61681V
- [14] Punning A, Kruusmaa M and Aabloo A 2006 Surface resistance experiments with IPMC sensors and actuators *Sensors Actuators A* **133** 200–9
- [15] https://www.ims.ut.ee/mediawiki/upload/6/69/IPMC_Mechanics_Algorithms.pdf (November 22, 2007)
- [16] Newbury K 2002 Characterization, modeling, and control of ionic polymer transducers *Dissertation* Virginia Polytechnic Institute and State University
- [17] Moreton H P 1992 Minimum curvature variation curves, networks, and surfaces for fair free-form shape design *PhD Thesis* University of California Berkeley
- [18] https://www.ims.ut.ee/mediawiki/upload/1/13/IPMC_Mechanics_Long.avi (November 22, 2007)
- [19] https://www.ims.ut.ee/mediawiki/upload/6/63/IPMC_Mechanics_Short.avi (November 22, 2007)

Q.4

Queries for IOP paper 245825

Journal: SMS
Author: M Anton et al
Short title: A mechanical model of a non-uniform IPMC actuator

Page 1

Query 1:

Author: Please be aware that the colour figures in this proof will normally only appear in colour in the online Web version. If you require colour in the printed journal and have not previously arranged it, please contact the Publishing Administrator now.

Page 5

Query A:

Author: If table 3 is not to be printed in colour, then please provide alternatives for the colour mentioned in column 1 of it.

Page 8

Query 2:

Author: Earlier, LabView 7 is referred to. Is this OK?

Page 10

Query 3:-

Author: Please check the alignment of equations in appendix B.

Query 4:-

Author: [11]: Any update?

Reference linking to the original articles

References with a volume and page number in blue have a clickable link to the original article created from data deposited by its publisher at CrossRef. Any anomalously unlinked references should be checked for accuracy. Pale purple is used for links to e-prints at ArXiv.